Motor imagery and self-recognition from actions

A. Kadambi, H. Lu, M. Monti, S. Narayanan, M. Iacoboni

PII: \$1053-8119(25)00528-2

DOI: https://doi.org/10.1016/j.neuroimage.2025.121525

Reference: YNIMG 121525

To appear in: Neurolmage

Received date: 26 May 2025

Revised date: 14 September 2025 Accepted date: 13 October 2025



Please cite this article as: A. Kadambi , H. Lu , M. Monti , S. Narayanan , M. Iacoboni , Motor imagery and self-recognition from actions, *NeuroImage* (2025), doi: https://doi.org/10.1016/j.neuroimage.2025.121525

This is a PDF file of an article that has undergone enhancements after acceptance, such as the addition of a cover page and metadata, and formatting for readability, but it is not yet the definitive version of record. This version will undergo additional copyediting, typesetting and review before it is published in its final form, but we are providing this version to give early visibility of the article. Please note that, during the production process, errors may be discovered which could affect the content, and all legal disclaimers that apply to the journal pertain.

© 2025 Published by Elsevier Inc. This is an open access article under the CC BY-NC-ND license (http://creativecommons.org/licenses/by-nc-nd/4.0/)

Highlights

- Motor imagery ability influences how the brain represents and recognizes one's own movements.
- Distinguishing the self from others using movement patterns can be decoded in brain regions linked to motor-based and action processing.
- Brain regions for body and social perception help identify people based on their motion patterns.



Motor imagery and self-recognition from actions

Kadambi A.^{1,2,3*}, Lu, H.^{2,4}, Monti, M.^{2,5}, Narayanan, S.⁶, Iacoboni, M.¹

- 1 Department of Psychiatry and Biobehavioral Sciences, Semel Institute for Neuroscience and Human Behavior, Brain Research Institute, David Geffen School of Medicine, University of California, Los Angeles, CA, USA
- 2 Department of Psychology, University of California University of California Los Angeles, Los Angeles, CA, USA
 - 3 Brain and Creativity Institute, University of Southern California, Los Angeles, CA, USA
 - 4 Department of Statistics, University of California Los Angeles, Los Angeles, CA, USA
 - 5 Department of Neurosurgery, Brain Research Center, David Geffen School of Medicine, University of California Los Angeles, Los Angeles, CA, USA 6 Google DeepMind, Zurich

*corresponding author

Email: akadambi@ucla.edu

Keywords: functional neuroimaging, self-recognition, body movements, action observation

Abstract

We recently identified cortical areas in the Action Observation Network that preferentially encoded self actions from minimal kinematic cues (Kadambi et al., 2025). Here, we investigate how identity decoding in these brain areas (Inferior Parietal Lobules, IPL; Inferior Frontal Gyri, IFG; Primary Motor Cortex, M1; Extrastriate Body Area, EBA; Superior Temporal Sulci, STS) relate to motor imagery ability. Using multivariate decoding and localizer analyses, we found that frontoparietal regions (IPL, IFG, and M1) selectively decoded self-identity, while occipitotemporal regions (EBA and STS), did not show such self-specific selectivity, but largely decoded across identities. Participant variability in motor imagery ability was positively associated with self-identity decoding in the IPL, EBA, STS and negatively with other-identity decoding in the IFG. These results introduce functional links between motor imagery and self-action decoding, emerging from frontoparietal and occipitotemporal regions.

1. Introduction

Our actions shape how we engage with the world and how we come to know it (Merleau-Ponty, 1945). While we have extensive visual experience observing the actions of others, third-person perspectives of our body movements are rare, and typically confined to mirrors or video recordings. Yet, from only around a dozen dots localized to key joints on the human body, humans can infer their own identity (Loula et al., 2005; Kadambi et al., 2024; Burling et al., 2019), as well as numerous high-level attributes from such visually sparse point-light displays (PLD)s, including action categories (Dittrich, 1993; van Boxtel & Lu, 2011), gender (Kozlowski and Cutting, 1977; Pollick et al., 2005), affect (Atkinson et al., 2004; Dittrich et al., 1996; De Gelder et al., 2015; Roether et al., 2009; Coulson, 2004), social intent (Manera et al., 2010; van Boxtel & Lu, 2012), and an innate sensitivity to visually sparse biological motion is observable even in newborns (Simion et al., 2003).

Self-recognition performance from PLDs depends on motor expertise. PLDs that involve more goal complexity (e.g., dancing) are better self-recognized than actions with less (e.g., waving; Loula et al., 2005; Kadambi et al., 2024, 2025; Burling et al., 2019). Self-performed PLDs are also recognized better than visually familiar friends and in a viewpoint invariant manner, in contrast to the viewpoint dependence observed for visually familiar others (Jokisch, Daum, & Troje, 2006). Beyond explicit visual recognition, this self-advantage extends across various domains, including implicit recognition of body parts (e.g., Frassinetti et al., 2011), action outcome prediction (e.g., Knoblich and Flach, 2001), facial expression decoding (Cook et al., 2012), memory for self-performed action verbs (Engelkamp and Krumnacker, 1980; see enactment effect), and multimodal action recognition (e.g., Repp and Knoblich, 2004; Flach et al., 2004; Murgia et al., 2012; Kennel et al., 2014).

Since PLDs only depict sparse visual information, the observed self-recognition advantage may be further attributed to non visual, potentially motoric factors (see Tsakiris 2010 for a review). A plausible candidate to support self-action recognition is motor imagery, or the motor simulation of movement without overt action execution (Jeannerod 2006). Motor imagery is implicated in well-known theories of action processing and in both the biological motion perception and self-recognition literature (Casile & Giese, 2006; Miller & Saygin, 2013; Kadambi et al., 2024). From systems-level brain imaging data, motor imagery engages partially overlapping neural substrates with motor execution—particularly in premotor and parietal cortices (Hardwick et al., 2018; Grezes and Decety, 2001; Caspers et al., 2010)—which could bridge action perception and self-identification (Iacoboni and Dapretto, 2006). Individuals with greater motor imagery ability also perform better on various biological motion tasks. These tasks include: discriminating the movement direction of a moonwalking point-light walker (Miller and Saygin, 2013) and improved motor learning from action observation (Lawrence et al., 2013), as well as

in self-action recognition studies from PLDs (Kadambi et al., 2024). Engaging in motor imagery also increases the degree of activity in these brain regions during action observation (Eaves et al., 2016). If motor imagery indeed facilitates biological motion perception, it may then be an especially important mechanism for mapping motor experience to self-action recognition.

A related open question is how motor imagery relates to the neural basis of self-recognition from actions. In our recent neuroimaging study on self-recognition of PLDs (Kadambi et al., 2025), we observed greater engagement of frontoparietal regions during action observation, notably the inferior parietal lobule and inferior frontal cortex, which are often associated with action simulation functions. In contrast, occipito temporal (OT) regions, like the EBA, also generally engaged during body and action observation, showed non-specific engagement for all identities (self-actions, friend-actions, and stranger-actions). These occipitotemporal areas seem to encode intact, body-related features (e.g., both static and dynamic postural attributes related to the human body: Zimmermann et al., 2018; De Gelder and Solanas, 2021; Downing et al., 2006; Walbrin et al., 2019; Orgs et al., 2016). However, the EBA is also implicated in selfprocessing, such as bodily self-awareness (Vocks et al., 2010; Hodzic et al., 2009), agency (David et al., 2008), and preferences for one's own body (Myers and Sowden, 2008; Berlucchi and Aglioti, 2009). Additionally, the superior temporal sulcus (STS) is sensitive to biological motion processing (Grossman & Blake, 2001; Thurman et al., 2016) and social perception, such as imitation (Iacoboni et al., 2001), intention understanding (Saxe et al., 2004; Brass et al., 2007), valence (Verosky and Todorov, 2010; Candidi et al., 2015), and social interactions (Masson and Isik, 2021; Isik et al., 2017). The larger extent to which these regions contribute to self-recognition and their relation to motor imagery remains unknown.

To directly examine the role and neural basis of motor imagery in self-recognition, we employed multivariate pattern (MVPA) and functional localizer analyses on data collected in our recent study of self-action recognition (Kadambi et al., 2025). Across two sessions, we first recorded participants' body movements, along with their sex-matched close friend using a motion capture system and converted the movements to point-light displays. After a delay period (~2-3 weeks), the participants returned for the second session consisting of a self-recognition task with their motion captured actions applied during neuroimaging. The present work introduces two main advances beyond the original report. First, by employing ROI-based MVPA, we investigated whether activity patterns in frontoparietal and temporo-occipital regions relevant to action processing reveal finer-grained neural decoding for self- versus other-recognition. Second, we relate participants' self-reported motor imagery traits with neural decoding in these regions to examine whether motor imagery ability influences self-action recognition and its underlying neural basis.

2. Methods

2.1 Participants

Twenty right-handed undergraduates (M_{age} =20.55, SD_{age}=1.73; 12 females, 8 males) from around the University of California, Los Angeles area were recruited using convenience sampling. All participants were compensated for their time. All participants had normal or corrected vision, no physical disabilities, and were unaware of the study's purpose. Sample size was determined based on prior fMRI studies using point-light biological motion (Saygin et al., 2004; Chang et al., 2021; Engelen et al, 2015) and self-generated point-light displays (Bischoff et al., 2012). The study was approved by the UCLA Institutional Review Board.

2.2 Apparatus

In order to capture participants' movements for the self-recognition task, we used the Microsoft Kinect V2.0 and Kinect SDK for motion capture, consistent with prior research on self-action recognition (Kadambi et al., 2024; Burling et al., 2019). Key joint coordinates in three dimensions (X-Y-Z) were recorded at ~33 frames per second. Each action sequence began and ended with a T-position signaled by the participant and was standardized in scale for the experiment. The action stimulus displayed in the experiment did not include the T-position. To reduce occasional frame-to-frame noise jitter, manual corrections were applied by replacing problematic frames with the preceding stable frame. Custom software from our lab was used for action processing and smoothing (Van Boxtel & Lu, 2013).

2.3 Stimuli

Twelve actions (argue, wash windows, get attention, hurry up, stretch, play guitar, jumping jacks, basketball, digging, chopping, laughing, directing traffic) were selected from our previous work on self-action recognition (Burling et al., 2019; Kadambi and Lu, 2019; Kadambi et al., 2024). These actions convey a range of variability in terms of action planning. PLDs were created using the above method for each participant, a sex-matched friend, and a sex-matched stranger. The stranger's action was randomly selected from one of three possible distractors for each sex (six total), pre-captured from actions of two of the experimenters and research assistants.

Six of the actions (i.e., argue, wash windows, get attention, hurry up, stretch, and play guitar) were categorized as "verbally instructed actions", based on a high degree of motoric goal complexity, as defined in our previous work (Burling et al., 2019; Kadambi et al., 2024). These actions were verbally instructed by the experimenter to the participant (e.g., "Please perform the action: 'to argue'). The remaining six actions were visually instructed by showing participants videos of actions performed by a stick figure. These actions were selected from the Carnegie Mellon Graphics (CMU) Motion Capture Database available Lab online (http://mocap.cs.cmu.edu) and depicted a range of goals (i.e., jumping jacks, basketball, digging,

chopping, laughing, directing traffic). To perform the visually instructed actions, participants first observed videos selected from the CMU dataset, with a stick figure performing an action without any verbal label provided. Then, they were instructed to imitate the movements of the action. The categorization of the action types, in addition to providing variability of the action goal, allowed us to further explore secondary analyses contrasting actions involving less motor familiarity due to copying someone else's motor plan (visual instruction) versus a different set of actions that involved more motor familiarity due to freely performing the action (verbal instruction).

2.4 Vividness of Motor Imagery Questionnaire

The Vividness of Movement Imagery Questionnaire-2 (VMIQ-2; Roberts et al., 2008) is a standardized psychometric survey measuring individual differences in the subjective vividness of motor imagery across three distinct imagery perspectives: internal visual imagery (first-person perspective), external visual imagery (third-person perspective), and kinesthetic imagery (felt experience of movement). The VMIQ-2 consists of 12 wholebody action items for each perspective, including kicking, running, and jumping, as well as fine motor tasks like writing and threading a needle. Participants are instructed to generate mental images of themselves performing each action and rate the clarity or vividness of these images using a five-point Likert scale, ranging from 1 ("Perfectly clear and as vivid as normal vision") to 5 ("No image at all, I only know that I am thinking of the movement"). Note that the scale is reversed scored, such that lower scores in VMIQ-2 indicate more vivid images and stronger motor imagery ability.

2.5 Procedure

Behavioral Session

Participants' body movements were recorded using the Microsoft Kinect V2.0 and Kinect SDK in a quiet testing room in Session 1. The Kinect was placed 1.5 m above the floor and 2.59 m away from the participant. Participants were instructed to perform the actions in a rectangular space to provide flexibility in how to perform the action while remaining within recording distance. Participants were instructed to naturalistically perform 12 different actions as described above and recorded by our motion capture system. They signaled the start and stop of action performance by performing an outstretched T-pose with their arms. Participant actions were then recorded and converted to point-light stimuli for use in the fMRI session.

Each of the 20 participants also brought a close friend of the same sex, who was separately recorded using the same paradigm. The recordings of the close friend were later used in the fMRI session to assess the impact of visual familiarity. None of the participants were informed

about the study's purpose on self-recognition but were provided a general description that the study examined visual action processing.

After the recording session, participants completed the Vividness of Motor Imagery-2 (VMIQ-2; Roberts et al., 2008) to measure motor simulation ability. Note that a few other attitudinal questionnaires, including the Autism-Spectrum Quotient (AQ; Baron-Cohen et al., 2001), Schizotypal Personality Questionnaire (SPQ; Raine, 1991) were also administered during Session 1 but were not included in the analyses reported here.

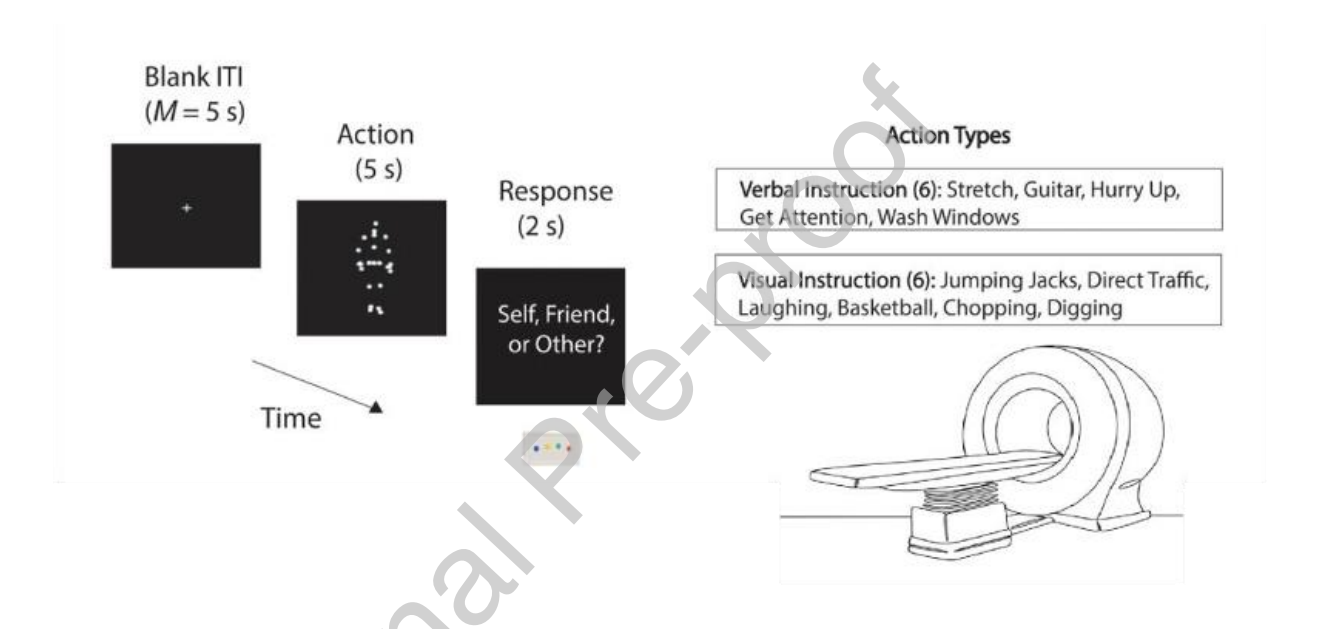


Figure 1. Trial structure including timing. Participants centrally attended to a white fixation cross until the action (self/friend/other) appeared for 5 s. On a subsequent screen, participants had 2 s to make their identity judgment, followed by the variable ITI (mean-centered at 5 s). The response order of self, friend, other was counterbalanced to reduce any impact of motor order.

fMRI session

After a delay period of around two-three weeks (mean delay days=18.55, SD=2.87), participants returned for brain imaging in Session 2. The total duration of the fMRI session lasted approximately 47 minutes, which included: initial acquisition scans (\sim 5 minutes), localizer task (\sim 8 minutes), self-recognition task (\sim 24 minutes), and resting state scan (\sim 10 minutes).

After initial brain acquisition scans, participants underwent functional localization. Two separate functional localizer scans were collected for posterior superior temporal sulcus (pSTS); Grossman et al., 2000; Grossman et al., 2010) and extrastriate body area (EBA; Peelen &

Downing, 2005; Downing et al., 2006; Downing et al., 2001). Each localizer was presented in a block design with alternating blocks of target and contrast stimuli, separated by jittered fixation intervals.

For the pSTS localizer, we used a standard biological motion functional localizer (Grossman et al., 2000) in which observed PLDs composed of 12 dots, globally constructed to perform 12 different everyday actions (e.g., jumping, kicking, running, throwing). While our main task, by contrast, used 25-dot PLDs (including fingers and additional joints) to maximize visual information for identity recognition, the localizer served only to define independent ROIs linked to biological motion, not to match stimuli and remained consistent with standard 12-dot PLDs (e.g., Grossman et al., 2000; Saygin et al., 2004). Participants also observed spatially scrambled PLDs in which the individual local dot trajectories of the point-light display remained intact, but the global configuration of the point lights was randomly displaced by randomizing the starting positions of the dots. Sensitivity to intact biological motion was contrasted with spatially scrambled biological motion for the task contrast of interest. Stimuli were displayed at 40 frames per second. Each trial lasted approximately 2 seconds followed by a jittered fixation period. The run included 12 alternating stimulus blocks (6 intact PLDs, 6 scrambled PLDs), interleaved with fixation periods (3 TRs), for a run duration of approximately 4 minutes.

For the EBA localizer, we used a standard body localizer (Downing et al., 2001) in which participants viewed headless grayscale photographs of human bodies (target condition) or chairs (contrast). Images were identical in size (400x400) and presented sequentially for 300 ms, followed by a 450 ms fixation, with a stimulus onset asynchrony of 750 ms. Each block contained 7 images (~5.25 s), followed by a 6-second fixation interval (3 TRs). A total of 12 blocks (6 body, 6 chair) were presented in alternating order. The run duration was ~4 minutes.

To ensure attention, participants also performed a one-back repetition detection task during both localizers. On ~20% of trials, the same stimulus (PLD or image) was repeated in immediate succession within a block. Participants were instructed to press the left response button when they detected such a repetition.

After the localizer scans, participants underwent the self-recognition task. For each trial of the task, participants observed a point-light display consisting of 25 joints, localized to the: head (head, neck, clavicle; 3 dots), arm (biceps, elbows, wrists; 6 dots), hands (fingers; 6 dots), stomach (1 dot), hips (3 dots), knees (2 dots), and leg (shin, feet; 4 dots). Each point-light display either showed their own action (self), same-sex familiar friend, or same-sex stranger action for a five-second duration. The same-sex stranger was selected at random (out of two options) between participants. Once selected, this stranger was consistently used for all actions involved in the experiment for that participant.

Shown in Figure 1, participants observed the action for five seconds, and were then prompted to identify with a finger-press response on the button box with the right hand whether the action video shown was their own, friend, or stranger within a two-second maximum response period. Participants responded by pressing one of three keys, with the index finger on the first, the middle finger on the second, and the ring finger on the third key. One identity was assigned to each key, and identity-key mapping was counterbalanced across subjects. Response mapping of self/friend/stranger was randomized between participants to reduce effects of trial structure or motor preparation or planning demands.

Participants' response was followed by jittered intertrial intervals (ITI) mean-centered at five seconds. There were four runs per participant, each consisting of 36 trials (12 trials per identity condition) in an event-related design. Experimental conditions within each run were pseudorandomized to reduce stimulus autocorrelation related to order and sequence effects, as well as correlated noise such as scanner drift.

2.6 MRI Acquisition

Magnetic resonance imaging was conducted using the Siemens 3-Tesla Prisma Fit scanner at the Staglin IMHRO Center for Cognitive Neuroscience, equipped with a 32-channel head coil. Scanning parameters for the T1 MPRAGE included: repetition time=2000 ms, echo time=2.52 ms, voxel size=1.0 mm³ isotropic voxels. T2*-weighted Gradient Recall Echo sequence was used for functional scan acquisition. Scanning parameters for the main task included repetition time=700 ms, echo time=33 ms, voxel size=2.5 mm isotropic voxels, field of view=192 mm, and flip angle=70°. Scanning parameters for the localizer task included repetition time=2000 ms, echo time=33 ms, voxel size=2.5 mm isotropic voxels, field of view=192 mm, and flip angle=70°. Four dummy scans were acquired and discarded before each scan to account for scanner stabilization. Participants underwent four runs of 36 trials each, with each run lasting approximately 360 seconds. Five dummy scans were acquired and discarded for the localizer tasks. All stimuli were presented on a projector and viewed through a mirror mounted on the head cover in the scanner.

2.7 ROI Creation

Functional Localizer ROIs

To localize the extrastriate body area (EBA), we measured the functional activation from the task contrast *bodies>chairs* elicited by the functional localizer in native space, uncorrected p<.05. Given the widespread activity evoked by the contrast, we constrained activity to the anatomical parcellation of the inferior lateral occipital cortex (LOC) from the Harvard-Cortical atlas

generated

by

FSLEYES

(https://fsl.fmrib.ox.ac.uk/fsl/fslwiki/Atlases) and thresholded the mask to include the top 70%

of voxels. The identical procedure was used for the posterior superior temporal sulcus (pSTS), with functional activation of interest measured by the contrast of intact>scrambled PLD and then constrained to the anatomical parcellation of the posterior superior temporal gyrus from the Harvard-Cortical Atlas. We used localizers specifically for the occipitotemporal regions since these regions are well-suited for stimulus-driven localizers (e.g., faces, bodies, objects), and isolate the relevant category-selective cortex. Importantly, functional localizers increase sensitivity and specificity since they are based on each participant's actual activation pattern. This is especially important in the occipitotemporal regions, since functional topography varies substantially across individuals in these regions.

Meta-analysis ROIs

ROIs for MVPA in the inferior parietal lobule (IPL) and inferior frontal gyri (IFG) were constrained to spherical regions implicated in bodily self-processing and action processing based on peak coordinates drawn from an activation likelihood estimation meta-analysis of action observation and imitation (Grosbras et al., 2012). In total, the meta-analysis incorporated over 90 fMRI and PET experiments (~993 subjects) and the studies included dynamic human stimuli (e.g., videos, point-light displays) and excluded overt movement, motor imagery, emotional behaviors, or clinical populations. Voxel-wise ALE maps were computed to estimate convergence of activation probability across studies, and the reported peak coordinates served as the basis for our ROI definitions. When the meta-analysis reported a region in only one hemisphere, we generated the contralateral ROI by inverting the x-coordinate. While the metaanalysis did not include the primary motor cortex (M1), we also included M1 using peak coordinates from our prior study which identified the M1 as an important site for self-identity decoding (Kadambi et al., 2025). Importantly, since the M1 peak was derived from the same dataset as Kadambi et al., 2025, we define the M1 as a hypothesis-driven ROI (rather than an independent ROI). We do not interpret the ROI in detail. For the coordinate-based ROIs, we accounted for individual variability in the peak ROI location by defining a sphere of 3-mm radius centered around the meta-analytic coordinate and moved the sphere within 4 voxels in each x,y,z direction for each participant as a ROI selection step. After exploring the search space, we then identified the ROI that produced the peak response for (self > friend and self > stranger) at the group-level. We then conducted the final MVPA with this peak coordinate. See Table 1 for a list of all coordinates used.

2.8 Imaging Analyses

Univariate Analysis

All univariate results are reported in Supplementary Materials and Kadambi et al., (2025). For the purposes of this article, we focus on the multivariate and functional localizer analyses and results.

Multivariate Analysis (MVPA)

Region of interest (ROI)-based MVPA was implemented using the CoSMoMVPA toolbox (http://www.cosmomvpa.org/; Oosterhof et al., 2016) in MATLAB R2020a. Regressors were defined based on the onsets and durations of the three experimental conditions (self-actions, friend-actions, or stranger-actions). Using the Least-Squares Separate approach, beta-series parameter estimates (Rissman, Gazzaley, & D'Esposito, 2004; Mumford et al., 2012) were iteratively estimated per trial by modeling a regressor for the event of interest in the trial and a regressor for all other events within the run. Standard motion parameters were also included as regressors in each trial-wise GLM. Preprocessing was identical to the univariate analysis, but no smoothing was applied. For each run, we extracted the 36 beta weights from each participant, normalized each beta weight within run, computed the average for each of the 36 action targets across all runs, and then demeaned the data (i.e., subtraction of the grand mean of all averaged targets from each averaged target). A linear support vector machine (SVM) was trained on neural activity patterns from three runs and tested on the remaining one run using the leave-one-run-out cross-validation measure for each participant.

Table 1. ROI Coordinates used for MVPA. The original location refers to the meta-analytic coordinate. New peak refers to the peak coordinate identified in the grid search space.

ROI Name	Original Location (x, y, z)	New Peak (x, y, z)
IFG RH	54, 28, 18	54, 30, 20
IFG LH	-54, 28, 18	-54, 28, 20
IPL RH	44, -56, 16	36, -56, 16
IPL LH	-44, -56, 16	-48, -52, 18
M1 RH	30, -23, 56	28, -22, 64
M1 LH	-30, -23, 56	-38, -20, 64

Note: EBA and STS regions were determined from functional localizer activation

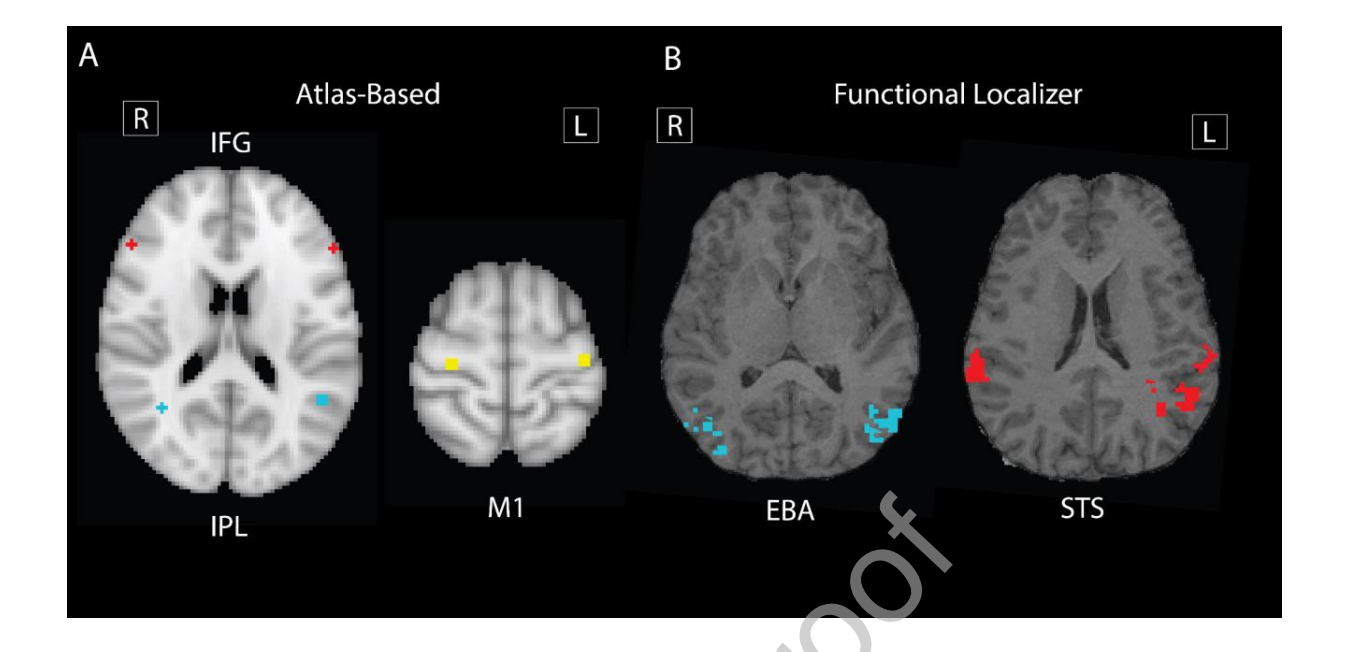


Figure 2. Regions-of-interest (ROIs) used for multivariate pattern analyses (MVPA). Panel A depicts Inferior Frontal Gyri (IFG) and Inferior Parietal Lobule (IPL) coordinates (from Grosbras et al., 2012) and M1 defined from our prior work (Kadambi et al., 2025). Red ROIs indicate the IFG, blue indicates IPL, and yellow indicates primary motor cortices (M1). Panel B depicts functional ROIs from a sample participant. The functional localizer ROIs were identified using functional localizer activity intersected with ROI-based anatomical masks from the Harvard-cortical atlas. The top 70% voxels were selected for each respective functional ROI.

Multiple Regression Analysis

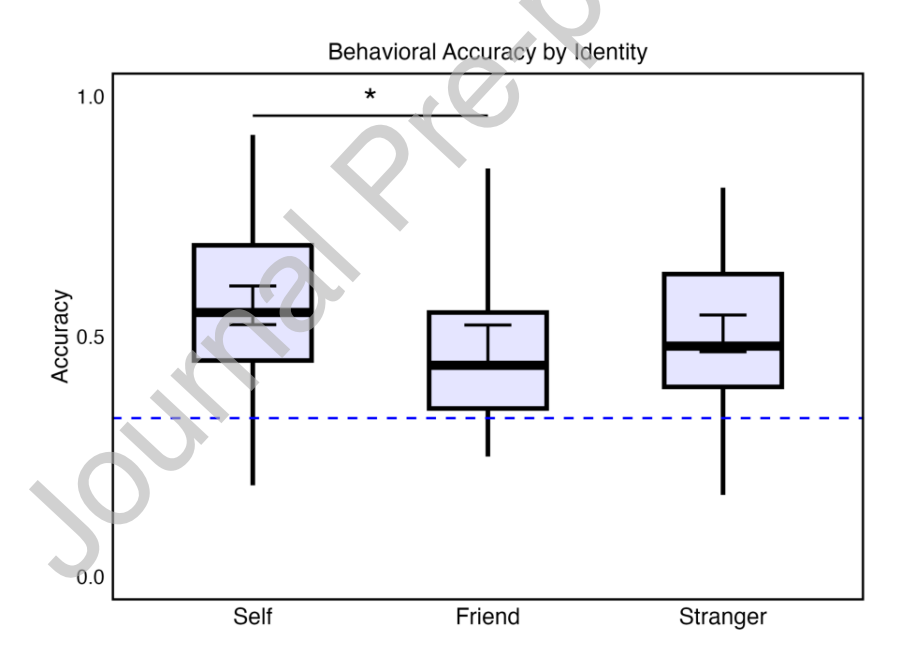
To measure associations between motor imagery ability and identity decoding, we employed backwards multiple regression analyses as a predictor selection step (using all VMIQ-2 subscales: kinaesthetic, internal, and external motor imagery) and follow-up Pearson correlations. The purpose of conducting independent, follow-up correlations was to ensure veridical relationships. Specifically, if we could not replicate the multiple regression analysis in post-hoc correlations, this could suggest that the results depend on the presence of other predictors in the model. However, if the predictor emerges significantly from the regression model and subsequently confirmed by separate bivariate correlations, the convergence strengthens confidence that the relationship reflects a genuine effect. Mean multivariate decoding accuracies were extracted from regions of interest for each two-class identity decoding (self vs stranger, self vs friend, friend vs stranger) and set as outcome variables. Multicollinearity was assessed using the Variance Inflation Factor (VIF). All predictors satisfied VIF criteria (no predictors had VIFs >5). Model significance was assessed using p-value significance and adjusted R^2 to balance parsimony and explanatory variance. To account for multiple comparisons, p-value significance between models was adjusted using a threshold

impinged on significant models (p>0.05), with the Benjamini-Hochberg False Discovery Rate. Unstandardized coefficients and 95% confidence intervals were reported in the final model. For non-significant associations, we report the lowest non-significant p-value model.

3. Results

3.1 Behavioral Results

First, we examined self-recognition accuracy in the visually sparse point-light displays. As previously reported in Kadambi et al (2025), one-sample t-tests revealed that participants could discriminate all identities (self, friend, stranger) significantly above chance (.33), self: M=.563, SD=.180, t(19)=5.789, p<.001, cohen's d=1.29; friend: M=.483, SD=.182, t(19)=3.754, p=.001, d=.839; stranger: M=.5052, SD=.172, t(19)=4.554, p<.001, d=1.01 (Figure 3). Pairwise t-tests corrected using Tukey's HSD revealed that self-generated actions (M=.563, SD=.180) were recognized significantly greater than friends' actions (M=.483, SD=.182), t(19)=2.673, p=.192. No difference was observed between recognition of friends' vs strangers' actions,



t(19)=-.454, p=.655.

Figure 3. Behavioral results of identity recognition accuracy. Mean recognition accuracy for each identity. Box plots denote that all identities were recognized significantly above chance (.33). Middle horizontal line reflects the median accuracy value. The upper and lower edges of each box denote the interquartile range, while the whiskers extend to the minimum and maximum observed values (1.5 times the interquartile range). Self actions were recognized significantly better than friend actions, and non-significant compared to strangers. No significant difference was observed between friends and strangers.

Error bars indicate the standard error of the mean (SEM). The horizontal dashed blue line indicates chance-level recognition accuracy (.33). * p < .05, ** p .01, *** p .001.

A significant interaction effect between action type and identity was also observed for self-generated actions, F(2,19)=7.546, p=.002, $\eta_p^2=.284$, revealing an effect of motor planning: actions generated by one's own motor plan (i.e., verbally instructed; M=.615, SD=.198) were better recognized relative to actions that were performed by copying someone else's motor plan (visually instructed, M=.513, SD=.189), t(19)=3.170, $p_{adj}=.049$, d=.709. Motor planning did not modulate recognition accuracy for any of the other identities, friends t(19)=.340, p=.999, nor strangers, t(19)=-2.195, p=.285. All post-hoc comparisons were corrected using Tukey's HSD. These results confirm action identity could be distinguished in the sparse visual displays, with an advantage for actions generated with one's own motor plan. Additional behavioral analysis on the individual actions are reported in Kadambi et al (2025).

3.2 Region-of-Analysis (ROI) Multivariate Pattern Analysis

Next, we used independently derived ROI-based MVPA to measure two-class decoding accuracy between each identity (self, friend, stranger) in the bilateral Extrastriate Body Area (EBA), Superior Temporal Sulcus (STS), Inferior Parietal Lobule (IPL), Inferior Frontal Gyri (IFG), and Primary Motor Cortices (M1) computed using one sample t-tests relative to chance performance (.50). We corrected for multiple comparisons using the false discovery rate (FDR) (Benjamini & Hochberg, 1995) on the number of ROIs (10 ROIs; *q*<.05). Specifically, for coordinate selection on the meta-analytic ROIs, we used the grid-search approach to identify the mean peak coordinate. The grid-search approach aimed to accounted for individual variability in the peak ROI location by defining a sphere of 3-mm radius centered around a meta-analytic coordinate (Grosbras et al., 2012) within a range of +/- 4 voxels in 3D space for each participant as a ROI selection step. After exploring the search space, we then identified the ROI that produced the peak response for (*self* > *friend* and *self* > *stranger*) at the group-level. The final MVPA was conducted with this peak coordinate. For coordinate selection on the functional localizers, we used the ROI generated from the localizer analysis. A summary of decoding results are referenced in **Table 2**.

3.2.1 Frontoparietal regions: Inferior Parietal Lobule and Inferior Frontal Gyrus decode self identity

We examined classification decoding accuracy in the frontoparietal regions ($Fig\ 4$, $Top\ Panel$) using one-sample t-tests against chance performance (0.5) and corrected for multiple comparisons using FDR. For the IPL (left: x,y,z=-48,-52,18; right: x,y,z=36,-56,16), we found selective decoding accuracy for the self from other identities in the left hemisphere: self v friend, $M_{\text{classification}}=.566$, t(19)=3.608, $p_{adj}=.008$, 95% CI [.0280, .1054], cohen's d=.807; self v stranger, $M_{\text{classification}}=.544$, t(19)=4.087, $p_{adj}=.006$, 95% CI [.0218, .0675], d=.914. No significant decoding accuracy was found for friend vs stranger, $M_{\text{classification}}=.503$, t(19)=.271,

 p_{adj} =.816, 95%CI [-.249, .992], d=.061. For the right IPL, we found significant decoding accuracy for self v stranger, $M_{\text{classification}}$ =.5323, t(19)= 2.730, p_{adj} =.0284, 95% CI [.0075, .0571], d=.610 and marginal for self v friend, $M_{\text{classification}}$ =.541, t(19)=2.224, p_{adj} =.0631, 95% CI [.0025, .0809], cohen's d=.497. No significant decoding accuracy was found for friend vs stranger, $M_{\text{classification}}$ =.5224, t(19)= 1.80, p_{adj} =.1315, 95%CI [-.0036, .0483], d=.403.

For the IFG (left: x,y,z=-54,28,20; right: x,y,z=54,30,20), the self could be selectively decoded from other identities in the right hemisphere: self v friend, $M_{\text{classification}}=.5459$, t(19)=2.763, $p_{adj}=.0284$, 95% CI [.131, 1.091], cohen's d=.618; self v stranger, $M_{\text{classification}}=.5313$, t(19)=2.445, $p_{adj}=.0488$, 95% CI [.069, 1.011],d=.547. No significant decoding accuracy was found for friend vs stranger, $M_{\text{classification}}=.517$, t(19)=1.641, $p_{adj}=.816$, 95% CI [-.091, .816], d=.367. We did not find significant identity decoding in the left hemisphere (self v friend, $M_{\text{classification}}=.5125$, t(19)=1.082, $p_{adj}=.3512$, 95% CI [.0017, 0367], cohen's d=.242; self v stranger, $M_{\text{classification}}=.5207$, t(19)=2.261, $p_{adj}=.0631$, 95% CI [.033, .966], d=.506; friend v stranger, $M_{\text{classification}}=.492$, t(19)=-.787, $p_{adj}=.5088$, 95% CI [-.615,.268], d=-.176.

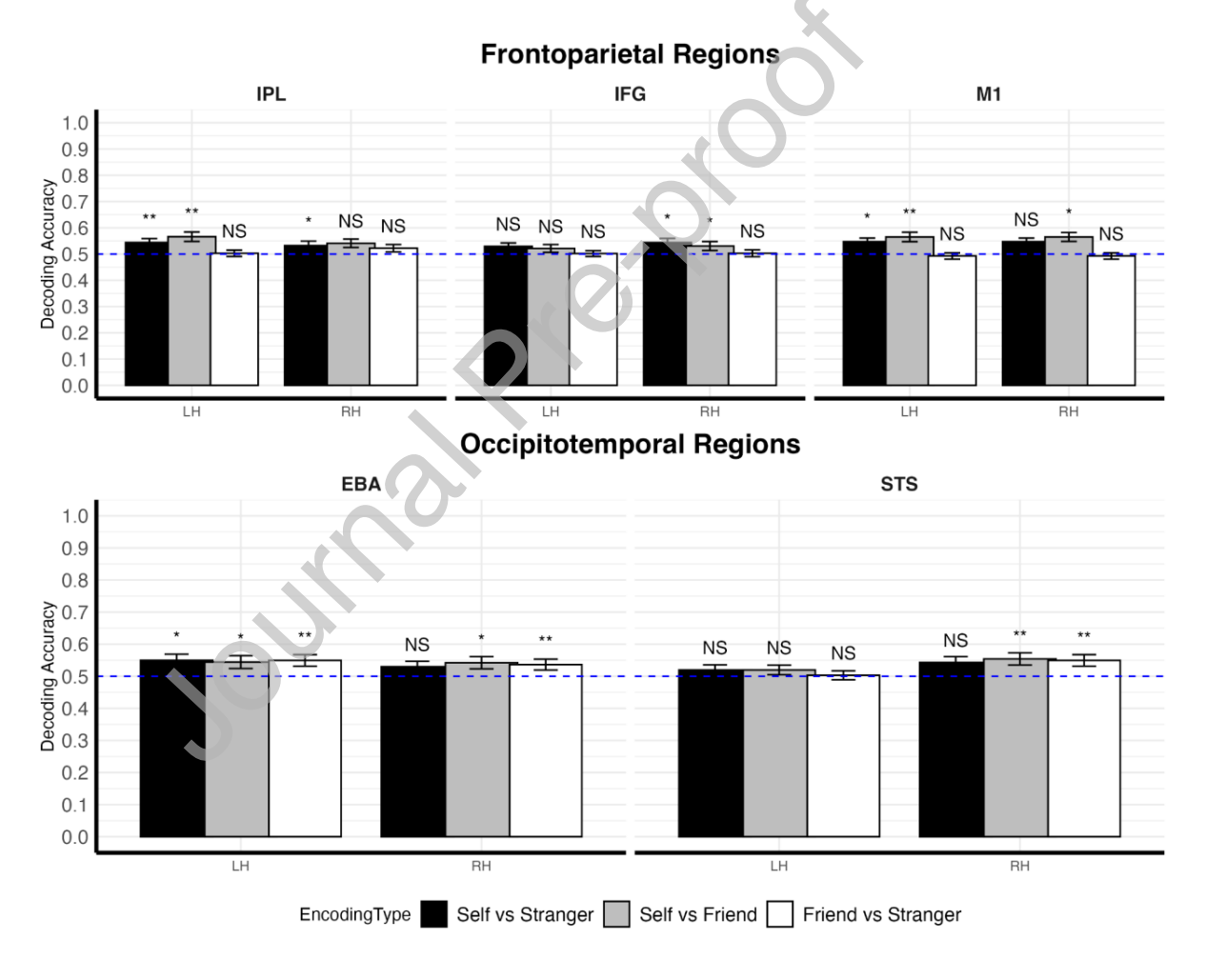
For the M1 (left: x,y,z=-38,-20,64; right: x,y,z=28,-22,64), we found selective decoding accuracy for the self in the left hemisphere: self v friend, $M_{\text{classification}}=.5651$, t(19)=4.631, $p_{adj}=.0043$, 95% CI [.0357, .0945], cohen's d=1.035; self v stranger, $M_{\text{classification}}=.5469$, t(19)=3.229, $p_{adj}=.0165$, 95% CI [.0165, .0772], d=772. No significant decoding accuracy was found for friend v stranger, $M_{\text{classification}}=.4927$, t(19)=-.651, $p_{adj}=.5184$, 95% CI [.0310, .0163], d=-.146. For the right hemisphere, we found significant decoding accuracy for self v friend, $M_{\text{classification}}=.536$, t(19)=3.112, $p_{adj}=.0189$, 95% CI [.198, 1.179], d=.696. No significant decoding accuracy was found for self v stranger, $M_{\text{classification}}=.5193$, t(19)=1.141, $p_{adj}=.3348$, 95% CI [-.194, .698], d=.255; triend v stranger, $M_{\text{classification}}=.5047$, t(19)=.398, $p_{adj}=.7442$, 95% CI [-.351, .527], d=.089.

3.2.2 Occipitotemporal regions: EBA decodes between all identities and STS decodes between friend identity

We next examined classification decoding accuracy in the occipitotemporal regions (*Figure 4*, *Bottom Panel*) using one-sample t-tests against chance performance (0.5) and corrected for multiple comparisons using FDR. For the EBA, significant decoding accuracy was observed for all identities (though note that self v stranger in the right EBA did not survive multiple comparisons correction). In the left EBA: self v friend, $M_{\text{classification}}$ =.5443, t(19)=2.881, p_{adj} =.0225, 95% CI [.0121, .0764], cohen's d=.644; self v stranger, $M_{\text{classification}}$ =.5499, t(19)=3.069, p_{adj} =.0189, 95% CI [.0159, .0839], d=.686; friend v stranger, $M_{\text{classification}}$ =.5495, t(19)=3.675, p_{adj} =.0075, 95% CI [.0213, .0777], d=.882. In the right EBA: self v friend, $M_{\text{classification}}$ =.5422, t(19)=2.912, p_{adj} =.0225, 95% CI [.0119, .0725], cohen's d=.651; self v

stranger, $M_{\text{classification}}$ =.5297, t(19)=2.246, p_{adj} =.0631, 95% CI [.0020, .0574],d=.502; friend v stranger: $M_{\text{classification}}$ =.5364, t(19)=3.579, p_{adj} =.0085, 95% CI [.0151, .0577], d=.800.

For the STS localizer, significant decoding accuracy was observed in the right hemisphere for some identity comparisons, but none for the left hemisphere. In the right STS: self v friend, $M_{\text{classification}}$ =.5541, t(19)=3.716, p_{adj} =.0084, 95% CI [.0236, .0845], cohen's d=.831; self v stranger, $M_{\text{classification}}$ =.5432, t(19)=2.194, p_{adj} =.2204, 95% CI [.0020, .0845];d=.491, friend v stranger, $M_{\text{classification}}$ =.5495, t(19)=3.675, p_{adj} =.0043, 95% CI [.0213, .0777], d=.882. In the left STS: self v friend, $M_{\text{classification}}$ =.5197, t(19)=1.522, p_{adj} =.1971, 95% CI [.0074,.0469], cohen's d=.340; self v stranger, $M_{\text{classification}}$ =.5197, t(19)=1.430, p_{adj} =.2204, 95% CI [-.0091,.0484], d=.320, friend v stranger, $M_{\text{classification}}$ =.5031, t(19)=.177, p_{adj} =.895, 95% CI [-.0331,.0392],



d=.040.

Figure 4. Decoding accuracies by identity. *Top Panel:* Decoding accuracies in frontoparietal regions showed a degree of selectivity for the self. The Left Inferior Parietal Lobule (IPL), Right Inferior Frontal

Gyrus (IFG), and Left Primary Motor Cortex (M1) significantly decoded self-identity relative to all other identities. Bottom Panel: Decoding accuracies in occipitotemporal regions. The Left Extrastriate Body Area (EBA) decoded between all identities, and the Right STS significantly decoded friend identity (friend vs stranger and friend vs self) significantly better than other comparisons. Dashed blue line indicates chance decoding accuracy (0.5). Error bars denote standard error of the means.

ROI decoding accuracies, N=20

Table 2. Decoding accuracies across ROIs after FDR correction.

	Self vs Stranger	Self vs Friend	Friend vs Stranger
IPL LH	t=4.087, p=0.00627	t=3.608, p=.00857	t=.271, p=.8164
IPL RH	t=2.730, p=.02847	t=2.224, p=.06315	t=1.800, p=.13159
IFG LH	t=2.261, p=.06315	t=1.082, p=.35124	t=787, p=.50884
IFG RH	t=2.445, p=.0488	t=2.763, p=.0284	t=1.641, p=.8164
M1 LH	t=3.229, p=.01653	t=4.631, p=.00436	t=651, p=.5184
M1 RH	t=1.141, p=.3348	t=3.112, p=.01893	t=.398, p=.74428
EBA LH	t=3.069, p=.01893	t=2.881,p=.0225	t=3.675, p=.0075
EBA RH	t=2.246, p=.06315	t=2.912, p=.0225	t=3.579, p=.0085
STS LH	t=1.430, p=.2204	t=1.522, p=.19718	t=.177, p=.895
STS RH	t=2.194, p=.06315	t=3.716, p=.0084	t=3.675, p=.00436

Boldface denotes statistical significance (corrected for multiple comparisons).

3.3 Relationships to motor imagery ability

Next, we measured whether decoding accuracy between identities in the ROIs related to motor imagery ability, using the VMIQ-2 subscale scores (internal, external, and kinaesthetic). Visual inspection of Q-Q plots revealed that raw scores on both internal and kinaesthetic motor imagery subscales deviated from normality (full analysis reported in Supplementary Materials). A Shapiro-Wilk test confirmed significant skew and leptokurtic data for internal motor imagery (W=0.826, p=0.002) and kinaesthetic motor imagery (skewness=1.3; kurtosis=4.75), W=0.86518, p=0.009678. Hence, we applied a Box–Cox transformation to both sets of scores. After the transformation, both skewness (internal: 0.17; kinesthetic: .081) and kurtosis (internal:

1.99; kinaesthetic: 2.045) significantly reduced, and the Shapiro–Wilk test yielded non-significant results (internal: W=0.942, p=0.265; kinaesthetic: W=0.95905, p=0.525), approximating a normal distribution. The transformed internal and kinaesthetic motor imagery scores were used in all subsequent analyses with the raw external motor imagery scores, which satisfied all assumptions. We related decoding accuracy in the ROIs with motor imagery ability in separate multiple regression models. Multicollinearity was assessed using the Variance Inflation Factor (VIF; all <5). We corrected for multiple comparisons between models using the Benjamini-Hochberg False Discovery Rate (Benjamini & Hochberg, 1995) based on hemisphere and site. Note all motor imagery (VMIQ-2) scores are reverse scored, in that higher scores indicate weaker motor imagery ability.

3.3.1 Frontoparietal regions: IPL decoding for self is associated with motor imagery ability For the Left IPL, the model showed that participants with more kinaesthetic (b=-1.582, p=.003, 95% CI [-2.534, -.630]) and reduced external (b=.004, p=.033, 95% CI [-2.097, 19.502]) motor imagery ability could better decode self from stranger identity, F(1,19)=7.184, $p_{adjusted}$ =.012, adjusted R^2 =.394 (shown in *Figure 5*; note that the scale for motor imagery is reverse-scored). Follow-up correlations confirmed the relationship between kinaesthetic motor imagery and Left IPL activity (r=-.535, p=.015, 95% CI [-.790, -.121]), while external motor imagery did not maintain significance (r=-.257, p=.274). No other significant models were observed: Left, self v friend, $p_{adjusted}$ =.301, friend v stranger, $p_{adjusted}$ =.301; Right, self v friend, $p_{adjusted}$ =.289; self v stranger, $p_{adjusted}$ =.383, friend v stranger, $p_{adjusted}$ =.289.

3.3.2 Frontoparietal regions: IFG decoding for other identities is negatively associated with motor imagery ability

For the Left IFG, we observed negative relationships between friend and stranger decoding and with internal motor imagery (b=5.297, p=.014, 95% CI [1.219, 9.376]), F(1,19)=7.445, $p_{adjusted}$ =.0420, adjusted R^2 =.253 (shown in Figure 5; note that the scale for motor imagery is reverse-scored). Follow-up correlation confirmed the relationship: r=.542, p=.013, 95% CI [.129, .794]. Note that kinesthetic motor imagery ability was also negatively associated with Left IFG activity (r=.501, p=.024, 95% CI [.076, .773]), but the coefficient did not attain significance during the initial predictor selection step, p=.241, p=.458. No significant models were observed for self vs friend p_{adjusted}=.250, self vs stranger p_{adjusted}=.316, nor the Right IFG: self v friend, p_{adjusted}=.204; self v stranger, p_{adjusted}=.358, friend v stranger, p_{adjusted}=.358.

Finally, while the regression model for Left M1 decoding self vs stranger actions was significantly predicted by internal motor imagery ability (p=.047), the model did not maintain significance after the FDR correction (p_{adjusted} =.141). No other significant regression models emerged for the M1: Left, p_{adjusted} =.704, friend vs stranger, p_{adjusted} =.704; Right, self v stranger: p_{adjusted} =.673, self v friend: p_{adjusted} =.469, friend vs stranger: p_{adjusted} =.156.

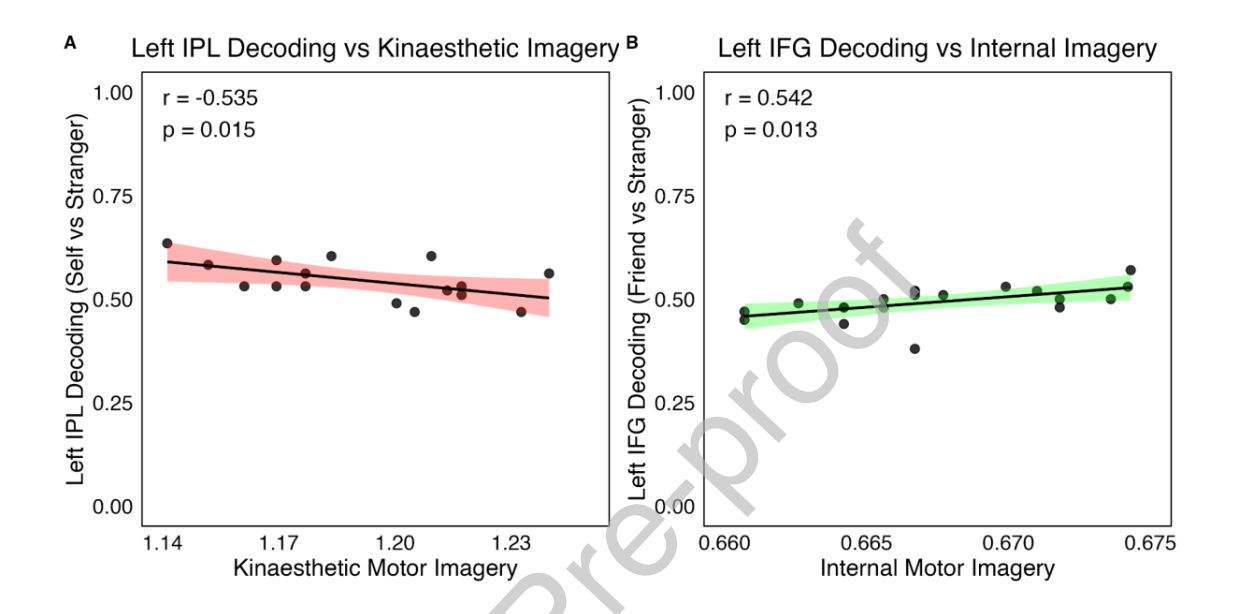


Figure 5. Associations between motor imagery (VMIQ-2) and identity decoding in frontoparietal regions: IPL and IFG. (A) Greater kinaesthetic motor imagery ability predicts better self vs stranger identity decoding accuracy in the left IPL (r=-.535,p=0.015). (B) Greater internal motor imagery ability predicts reduced friend vs stranger decoding in the right IFG (r=.542, p=.013). Each panel depicts individual data points (black dots), regression line (black), and 95% confidence interval. All y-axes represent decoding accuracy (0–1), while x-axes reflect motor imagery ability scores. Note: all VMIQ-2 scores measuring motor imagery are reverse-scored. Specifically, higher motor imagery scores on the VMIQ-2 indicate reduced motor imagery ability. The scores were transformed with a Box–Cox transformation .

3.3.3 Occipitotemporal regions: Left EBA decoding for self identity is associated with motor imagery ability

For the Left EBA, participants with more kinaesthetic motor imagery (b=-1.066, p=.005,

95% CI [-1.765, -.366]) better decoded self actions from friends' actions, F(1,19)=10.247, $p_{\text{adjusted}}=.012$, adjusted $R^2=.327$ (shown in Figure 6; note that the scale for motor imagery is reverse-scored). Follow-up correlations confirmed the relationship between kinaesthetic motor imagery and Left EBA activity (r=-.602, p=.005, 95% CI [-.825, -.218]), as well as with composite motor imagery scores (r=-.467, p=.038, 95% CI [-.754, -.031]). While the regression model for decoding friend from strangers actions was also significant in the Left EBA, $F(2,17)=6.476, p_{\text{adjusted}}=.012$, with external (b=.007, p=.013, 95% CI [.002, .012]) and

kinaesthetic (b=-2.019, p=.002, 95% CI [-3.220 -.817]) motor imagery, neither relationship maintained in follow-up correlations (kinaesthetic: r=-.412, p=.065; external: r=-.133, p=.635). No other significant models were observed: Left, self vs stranger ($p_{adjusted}$ =.051); Right, self vs friend ($p_{adjusted}$ =.289), self vs stranger ($p_{adjusted}$ =.383), friend vs stranger ($p_{adjusted}$ =.289).

3.3.4 Occipitotemporal regions: Left STS decoding for self identity is associated with motor imagery ability

For the Left STS, participants with more internal motor imagery ability better decoded self from stranger identities, b=-8.827, p=.009, 95% CI [-14.183, -.172], F(1,19)=8.719, $p_{adjusted}$ =.027, adjusted R^2 =.289 (shown in Figure 6; note that the scale for motor imagery is reverse-scored). Follow-up correlations confirmed the relationship between internal motor imagery and Left STS decoding accuracy (r=-.571, p=.009, 95% CI [-14.183, 2.391]). No other significant models were observed: Left, self vs friend ($p_{adjusted}$ =.507), friend vs stranger ($p_{adjusted}$ =.393), Right, self vs friend ($p_{adjusted}$ =.456), self vs stranger ($p_{adjusted}$ =.913), friend vs stranger ($p_{adjusted}$ =.456).

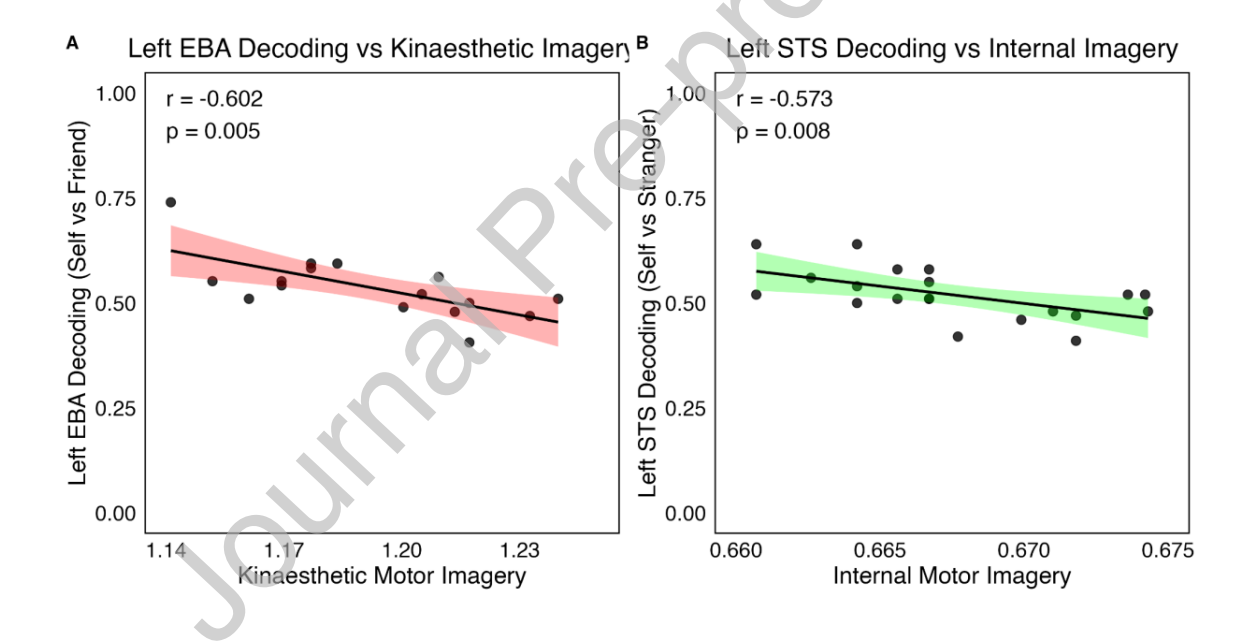


Figure 6. Associations between motor imagery (VMIQ-2) and identity decoding in occipitotemporal localizer regions: EBA and STS. (A) Greater kinaesthetic motor imagery ability predicts better self vs friend identity decoding accuracy in the Left EBA (r=-.602, p=0.005). (B) Greater internal motor imagery ability predicts better self vs stranger decoding in the Left STS (r=-.573, p=.008). Each panel depicts individual data points (black dots), regression line (black), and 95% confidence interval. All y-axes represent decoding accuracy (0–1), while x-axes reflect motor imagery ability scores. Note: all VMIQ-2 results are reverse-scored and transformed.

4. Discussion

Our findings demonstrate that brain areas involved in self-action recognition are influenced by motor imagery ability. Theories of action simulation posit that the ability to internally simulate motor actions underlies both the physical act of motor production as well as the perceptual observation of actions (Gallese and Goldman, 1998; Gallese, 2005). Consistent with this framework, our neuroimaging data demonstrate a key role of motor imagery, as a proxy for action simulation, in facilitating the neural decoding of self-action identity. These relationships were observed in the inferior parietal lobule (IPL), inferior frontal gyrus (IFG), primary motor cortex (M1), extrastriate body area (EBA), and superior temporal sulcus (STS).

Building on our prior work (Kadambi et al., 2025) which identified self-action recognition markers across the action observation network (broadly including frontoparietal and occipitotemporal regions), the present study extends those findings by linking multivariate decoding accuracy to motor imagery ability. These results introduce neural evidence for motor imagery ability as a possible mechanism to support self-recognition from actions.

A specific selectivity for self-action identity decoding was observed in the following frontoparietal sites: Left IPL, Left M1, and Right IFG. These regions are considered neural substrates for action simulation, and involved in discriminating between actions of the self and others (Rizzolatti & Craighero, 2004; Iacoboni, 2009). Moreover, the degree of activation in these regions is modulated by the observer's degree of motor familiarity and expertise (Calvo-Merino et al., 2006; Cross et al., 2006) and greater volume in these regions is associated with increased motor imagery ability (Furuta et al., 2024). Note that while we do not advance a strong claim regarding hemispheric lateralization due to modeling individual variability, we report hemispheric findings across all sites for completeness.

In the Left IPL, individuals with stronger kinaesthetic motor imagery, i.e., simulating the 'feeling' associated with motor execution, were better able to decode their own actions. The IPL is implicated in numerous processes, including visuospatial processing, motor attention, movement selection, motor planning (Binkofski and Buxbaum, 2013, Buxbaum et al., 2007, Lebon et al., 2012, Rizzolatti and Matelli, 2003, Rushworth et al., 2001, Rushworth et al., 1997), and bodily self-awareness (i.e., encoding the awareness of the body in space, Gallese et al., 2007). Damage to this region from stroke or with targeted inhibitory non-invasive brain stimulation impairs motor imagery ability (Oostra et al., 2016; Evans et al., 2016; Kraeutner et al., 2016, McInnes et al., 2016, Sirigu et al., 1996; Kraetner et al., 2019), which generally shows a left hemisphere dominance (Binkofski and Buxbaum, 2013; Buxbaum et al., 2007; Buxbaum et al., 2006; Evans et al., 2016). Our findings support the role of the IPL (notably the left) as a region encoding motor imagery as a key region supporting internal self-action representations.

In the occipitotemporal cortex, the Left EBA successfully decoded all identities, while the Right EBA and STS prioritized friend identity decoding. The EBA has been previously shown to distinguish between the self and others body representations, such as static photographs (Vocks et al., 2010). This differentiation, however, is not strictly self-specific and the EBA can distinguish across different identities (Chan et al., 2004), as is consistent with our data. Notably, decoding between self and friend actions that emerged in the Left EBA was associated with kinaesthetic motor imagery ability. The novel relationship with motor imagery suggests a deeper function of the EBA, potentially in integrating kinaesthetic and visuo-motor (internal) feedback to support the keeping of online, internal topographic body representations (Ishizu et al., 2009; Orlov et al., 2010). For instance, transiently inhibiting EBA activity is shown to reduce proprioceptive awareness of one's own limb (Wold et al., 2014), while applying excitatory direct current stimulation to the lateral occipital temporal cortex increases motor imagery ability (Kikuchi et al., 2017). The EBA also responds to participants' limb-directed movements, even when their eyes are closed (Astafiev et al., 2004), lending support to its role in internally generated, proprioceptive or motor-based representations, beyond visual processing alone.

For the Left STS, decoding accuracy between self and stranger was associated with internal motor imagery ability in the left hemisphere. The STS is a key site implicated in processing biological motion (Grossman & Blake, 2001) and action imagery (Kourtzi & Kanwisher, 2000). Unlike kinaesthetic motor imagery which involves imagining the sensations and feelings of actions, internal motor imagery reflects a more visuomotor perspective (i.e., a first-person visualization of performing the action). The association between STS decoding and internal motor imagery ability may therefore reflect the STS's role in supporting visual, rather than bodily, aspects of imagined action (Grossman & Blake, 2001). Note that lateralized patterns did emerge in our results. For instance, stranger and friend identity decoding was stronger in the right STS whereas motor imagery ability was associated with decoding self-identity in the left hemisphere counterpart. While we refrain from drawing strong conclusions about hemispheric specialization, this asymmetry may point to partially distinct roles for left and right hemisphere regions in processing identity-related versus imagery-related features.

While the Left IFG did not show significant identity decoding between identities, decoding between friend and strangers negatively related to internal motor imagery ability (i.e., the first-person simulation of action production). Specifically, individuals with more vivid internal motor imagery relied less on the IFG when differentiating between familiar (friend) and unfamiliar (stranger) actors. One possible interpretation may relate to previous work on action representations. That work suggested a division of labor according to which IFG codes more the goal of the action (Sokolov et al., 2018; Wurm et al., 2014) and the IPL its precise motor specification (Iacoboni et al., 2005). Therefore, IPL-based motor specification may go together with motor imagery to decode identities (friend versus stranger in this case), while IFG-based

goal processing may get in the way of decoding identities, since action goals can be achieved with many different motoric specifications. Note that across the correlation analyses between multivariate pattern analysis and motor imagery, a few participants scored below chance performance on identity decoding. However, no participants exhibited extreme or systematic below-chance decoding. Hence, we avoided excluding any participants with slightly below-chance decoding. These values are expected due to sampling variability around the chance baseline and excluding them could bias the results by removing valid variability.

Finally, while our sample size was modest (N=20), we employed rigorous analysis strategies, including variable transformations, regression modeling for predictor selection, and multiple comparisons correction. Nevertheless, we acknowledge the limitations of our sample size. Future work with larger cohorts can further substantiate and expand upon our findings.

4.1 Conclusions

Our results suggest that motor imagery and the process of self-recognition from visually sparse actions are functionally linked. Cortical areas involved in action processing for self and others appear to encode these functional links. Together, these findings support longstanding embodied frameworks (Merleau-Ponty, 1962; Gallagher, 2006) that have to date only speculated on the importance of motor imagery and action simulation in supporting self-action recognition. Future investigations can help determine the extent of its relevance to clinical disorders related to self-recognition, and interventions aimed at neurorehabilitation.

Acknowledgments

This project was supported by UCLA faculty research grant to H.L., Tiny Blue Dot Foundation grant to M.M.M., and APA Dissertation Award to AK. Preliminary versions of this project were presented at the Virtual Society for Neuroscience (2020), V-Vision Sciences Society (2020), Society for Neuroscience (2022), and Association for Scientific Study of Consciousness (2023). We thank Sophia Baia and Kelly Xue for assistance with data collection and stimuli creation, and Elinor Yeo, Jolie Wu, Kelly Nola, Nicolas Jeong, Danya Elghebagy, David Lipkin, Shahan McGahee for assistance with stimuli creation.

Data Availability: All analysis scripts, behavioral data, and results from the imaging analyses can be downloaded from our GitHub repository: https://github.com/akilakada/self-fmri. Raw nifti data can be shared upon request to the corresponding author and subject to the UCLA Institutional Review Board Guidelines.

Declarations. S.N. is an employee of Google DeepMind. Google DeepMind had no role in study design, data collection and analysis, decision to publish, or preparation of the manuscript. All other authors declare no competing financial interests.

References

- Astafiev, S. V., Stanley, C. M., Shulman, G. L., & Corbetta, M. (2004). Extrastriate body area in human occipital cortex responds to the performance of motor actions. Nature Neuroscience, 7(5), 542–548.
- Atkinson, A. P., Dittrich, W. H., Gemmell, A. J., & Young, A. W. (2004). Emotion perception from dynamic and static body expressions in point-light and full-light displays. Perception, 33(6), 717-746.
- Baron-Cohen, S., Wheelwright, S., Skinner, R., Martin, J., & Clubley, E. (2001). The autism-spectrum quotient (AQ): Evidence from Asperger syndrome/high-functioning autism, males and females, scientists and mathematicians. *Journal of Autism and Developmental Disorders*, 31(1), 5-17.
- Berlucchi, G., & Aglioti, S. M. (2009). The body in the brain revisited. Experimental Brain Research, 200(1), 25-35.
- Binkofski, F., & Buxbaum, L. J. (2013). Two action systems in the human brain. Brain and language, 127(2), 222-229.
- Bischoff M, Zentgraf K, Lorey B, Pilgramm S, Balser N, Baumgartner E, Hohmann T, Stark R, Vaitl D, Munzert J (2012). Motor familiarity: brain activation when watching kinematic displays of one's own movements. Neuropsychologia 50:2085–2092.
- Brass, M., Schmitt, R. M., Spengler, S., & Gergely, G. (2007). Investigating action understanding: Inferential processes versus action simulation. Current Biology, 17(24), 2117-2121.
- Burling, J. M., Kadambi, A., Safari, T., & Lu, H. (2019). The impact of autistic traits on self-recognition of body movements. Frontiers in Psychology, 9, 2687.
- Buxbaum, L. J., Kyle, K., Grossman, M., & Coslett, B. (2007). Left inferior parietal representations for skilled hand-object interactions: evidence from stroke and corticobasal degeneration. Cortex, 43(3), 411-423.
- Candidi, M., Stienen, B. M., Aglioti, S. M., & de Gelder, B. (2015). Virtual lesion of right posterior superior temporal sulcus modulates conscious visual perception of fearful expressions in faces and bodies. Cortex, 65, 184-194.
- Calvo-Merino B, Grèzes J, Glaser DE, Passingham RE, Haggard P (2006). Seeing or doing? Influence of visual and motor familiarity in action observation. Current Biology 16:1905–1910.
- Casile, A., & Giese, M. A. (2006). Nonvisual motor training influences biological motion perception. *Current Biology*, 16(1), 69–74.
- Caspers, S., Zilles, K., Laird, A. R., & Eickhoff, S. B. (2010). ALE meta-analysis of action observation and imitation in the human brain. *NeuroImage*, 50(3), 1148–1167.
- Chan, A. W., Peelen, M. V., & Downing, P. E. (2004). The effect of viewpoint on body

- representation in the extrastriate body area. Neuroreport, 15(15), 2407-2410.
- Chang DH, Troje NF, Ikegaya Y, Fujita I, Ban H (2021). Spatiotemporal dynamics of responses to biological motion in the human brain. Cortex 136:124–139.
- Cook, R., Johnston, A., & Heyes, C. (2012). Self-recognition of avatar motion: How do I know it's me? *Proceedings of the Royal Society B: Biological Sciences*.
- Coulson, M. (2004). Attributing emotion to static body postures: Recognition accuracy, confusions, and viewpoint dependence. *Journal of Nonverbal Behavior*, 28(2), 117–139.
- Cross, E. S., Hamilton, A. F. d. C., & Grafton, S. T. (2006). Building a motor simulation de novo: Observation of dance by dancers. *NeuroImage*, 31(3), 1257–1267.
- David, N., Cohen, M. X., Newen, A., Bewernick, B. H., Shah, N. J., Fink, G. R., & Vogeley, K. (2008). The extrastriate cortex distinguishes between the consequences of one's own and others' behavior. Neuroimage, 36(3), 1004-1014.
- de Gelder, B., & Poyo Solanas, M. (2021). A computational neuroethology perspective on body and expression perception. Trends in Cognitive Sciences, 25(9), 744-756.
- Dittrich, W. H. (1993). Action categories and the perception of biological motion. Perception, 22(1), 15-22.
- Dittrich, W. H., Troscianko, T., Lea, S. E., & Morgan, D. (1996). Perception of emotion from dynamic point-light displays represented in dance. *Perception*, 25(6), 727–738.
- Downing, P. E., Wiggett, A. J., & Peelen, M. V. (2006). Functional magnetic resonance imaging investigation of overlapping lateral occipitotemporal activations using multi-voxel pattern analysis. Journal of Neuroscience, 27(1), 226-233.
- Downing, P. E., Jiang, Y., Shuman, M., & Kanwisher, N. (2001). A cortical area selective
 - for visual processing of the human body. Science, 293(5539), 2470–2473.
- Eaves, D. L., Riach, M., Holmes, P. S., & Wright, D. J. (2017). Motor imagery during action observation: A brief review of evidence, theory and future research opportunities. Frontiers in Neuroscience, 10, 514.
- Engelen T, de Graaf TA, Sack AT, de Gelder B (2015) A causal role for inferior parietal lobule in emotion body perception. Cortex, 73-202.
- Engelkamp J., & Krumnacker H. (1980). Image- and motor-processes in the retention of verbal materials. [Image- and motor-processes in the retention of verbal materials.]. Zeitschrift Für Experimentelle Und Angewandte Psychologie.
- Flach, R., Knoblich, G., & Prinz, W. (2004). Recognizing one's own clapping: The role of temporal cues. *Psychological Research*, 69(4), 245–252.

- Furuta, T., Morita, T., Miura, G., & Naito, E. (2024). Structural and functional features characterizing the brains of individuals with higher controllability of motor imagery. Scientific Reports, 14(1), 17243.
- Gallagher, S. (2006). How the body shapes the mind. Clarendon press.
- Gallese, V. (2005) Embodied simulation: from neurons to phenomenal experience. Phenomenal. Cogn. Sci. 4, 23–48
- Gallese, V. (2007). The "conscious" dorsal stream: embodied simulation and its role in space and action conscious awareness. Psyche, 13(1), 1-20.
- Gallese, V. and Goldman, A.I. (1998) Mirror neurons and the simulation theory of mind-reading. Trends Cogn. Sci. 2, 493–551
- Grezes, J., & Decety, J. (2001). Functional anatomy of execution, mental simulation, observation, and verbal conceptualization of action. *NeuroImage*, 14(1), S112–S118.
- Grosbras, Marie Hélène, Susan Beaton, and Simon B. Eickhoff. "Brain regions involved in human movement perception: A quantitative voxel based meta analysis." Human brain mapping 33.2 (2012): 431-454.
- Grossman, E., Donnelly, M., Price, R., Pickens, D., Morgan, V., Neighbor, G., & Blake, R. (2000). Brain areas involved in perception of biological motion. Journal of cognitive neuroscience, 12(5), 711-720.
- Grossman, E. D., & Blake, R. (2001). Brain activity evoked by inverted and imagined biological motion. *Vision Research*, 41(10-11), 1475-1482.
- Grossman, E. D., Jardine, N. L., & Pyles, J. A. (2010). fMR-adaptation reveals invariant coding of biological motion on the human STS. *Frontiers in Human Neuroscience*, 4, 15.
- Haggard, P. (2005) Conscious intention and motor cognition. *Trends in Cognitive Sciences*, 9(6), 290–295.
- Hardwick, R. M., Caspers, S., Eickhoff, S. B., & Swinnen, S. P. (2018). Neural correlates
 - of action: Comparing meta-analyses of imagery, observation, and execution. *Neuroscience & Biobehavioral Reviews*, 94, 31–44.
- Hodzic, A., Kaas, A., Muckli, L., Stirn, A., & Singer, W. (2009). Distinct cortical networks for the detection and identification of human body. Neuroimage, 45(4), 1264-1271.
- Iacoboni, M. (2009). Imitation, empathy, and mirror neurons. *Annual Review of Psychology*, 60, 653–670.
- Iacoboni, M., Koski, L. M., Brass, M., Bekkering, H., Woods, R. P., Dubeau, M. C., ... & Mazziotta, J. C. (2001). Reafferent copies of imitated actions in the right superior

- temporal cortex. *Proceedings of the National Academy of Sciences*, 98(24), 13995–13999.
- Iacoboni, M., & Dapretto, M. (2006). The mirror neuron system and the consequences of its dysfunction. *Nature Reviews Neuroscience*, 7(12), 942–951.
- Iacoboni, M., Molnar-Szakacs, I., Gallese, V., Buccino, G., Mazziotta, J. C., & Rizzolatti, G. (2005). Grasping the intentions of others with one's own mirror neuron system. PLoS Biology, 3(3), e79.
- Isik, L., Koldewyn, K., Beeler, D., & Kanwisher, N. (2017). Perceiving social interactions in the posterior superior temporal sulcus. Proceedings of the National Academy of Sciences, 114(43), E9145-E9152.
- Ishizu, T., Noguchi, A., Ito, Y., Ayabe, T., & Kojima, S. (2009). Motor activity and imagery modulate the body-selective region in the occipital—temporal area: A nearinfrared spectroscopy study. Neuroscience Letters, 465(1), 85-89.
- Jeannerod, M. (2006). *Motor cognition: What actions tell the self.* Oxford University Press.
- Jokisch, D., Daum, I., & Troje, N. F. (2006). Self-recognition versus recognition of others by biological motion: Viewpoint-dependent effects. *Perception*, 35(7), 911–920.
- Kadambi, A., Xie, Q., & Lu, H. (2024). Individual differences and motor planning influence self-recognition of actions. PLoS ONE, 19(7), e0303820. Kadambi, A., Erlikhman, G., Johnson, M., Monti, M. M., Iacoboni, M., & Lu, H. (2025).
 - Self-awareness from whole-body movements. Journal of Neuroscience, 45(3).
- Kikuchi, M., Takahashi, T., Hirosawa, T., Oboshi, Y., Yoshikawa, E., Minabe, Y., & Ouchi, Y. (2017). The lateral occipito-temporal cortex is involved in the mental manipulation of body part imagery. Frontiers in Human Neuroscience, 11, 181.
- Kilner, J. M. (2011). More than one pathway to action understanding. Trends in Cognitive Sciences, 15(8), 352-357.
- Kraeutner, S. N., Keeler, L. T., & Boe, S. G. (2016). Motor imagery-based skill acquisition disrupted following rTMS of the inferior parietal lobule. Experimental Brain Research, 234(2), 397-407.
- Kraeutner, S. N., McWhinney, S. R., Solomon, J. P., Dithurbide, L., & Boe, S. G. (2019). Experience modulates motor imagery-based brain activity. European Journal of Neuroscience, 50(12), 3728-3739.
- Lebon, F., Lotze, M., Stinear, C. M., & Byblow, W. D. (2012). Task-dependent interaction between parietal and contralateral primary motor cortex during explicit versus implicit motor imagery. PLoS One, 7(5), e37850.

- Manera, V., Schouten, B., Becchio, C., Bara, B. G., & Verfaillie, K. (2010). Inferring intentions from biological motion: A stimulus set of point-light communicative interactions. *Behavior Research Methods*, 42(1), 168–178.
- Masson, H. L., & Isik, L. (2021). Functional selectivity for social interaction perception in the human superior temporal sulcus. bioRxiv.
- McInnes, K., Friesen, C., & Boe, S. (2016). Specific brain lesions impair explicit motor imagery ability: A systematic review of the evidence. Archives of Physical Medicine and Rehabilitation, 97(3), 478-489.
- Merleau-Ponty, M. (1962). Phenomenology of perception. Routledge.
- Miller, L. E., & Saygin, A. P. (2013). Individual differences in the perception of biological motion: Links to social cognition and motor imagery. *Cognition*, 128(2), 140–148.
- Myers, A., & Sowden, P. T. (2008). Your hand or mine? The extrastriate body area. Neuroimage, 42(4), 1669-1677.
- Naito, E., Morita, T., & Amemiya, K. (2016). Body representations in the human brain revealed by kinesthetic illusions and their essential contributions to motor control and corporeal awareness. Neuroscience research, 104, 16-30.
- Northoff, G. (2016). Is the self a higher-order or fundamental function of the brain? The "basis model of self-specificity" and its encoding by the brain's spontaneous activity. Cognitive Neuroscience, 7(1-4), 203-222.
- Oosterhof, N. N., Connolly, A. C., & Haxby, J. V. (2016). CoSMoMVPA: Multi-modal multivariate pattern analysis of neuroimaging data in MATLAB/GNU Octave. *Frontiers in Neuroinformatics*, 10, 27.
- Orgs, G., Dovern, A., Hagura, N., Haggard, P., Fink, G. R., & Weiss, P. H. (2016). Constructing visual perception of body movement with the motor cortex. Cerebral Cortex, 26(1), 440-449.
- Rizzolatti, G., & Craighero, L. (2004). The mirror-neuron system. Annu. Rev. Neurosci., 27(1), 169-192.

Roberts, R., Callow, N., Hardy, L., Markland, D., & Bringer, J. (2008). Movement

- imagery ability: Development and assessment of a revised version of the Vividness of Movement Imagery Questionnaire. *Journal of Sport & Exercise Psychology*, 30(2), 200–221.
- Saxe, R., Xiao, D. K., Kovacs, G., Perrett, D. I., & Kanwisher, N. (2004). A region of right posterior superior temporal sulcus responds to observed intentional actions. Neuropsychologia, 42(11), 1435-1446.
- Saygin AP, Wilson SM, Hagler DJ, Bates E, Sereno MI (2004) Point-light biological

- motion perception activates human premotor cortex. J Neurosci 24:6181-6188.
- Simion, F., Regolin, L., & Bulf, H. (2003). A predisposition for biological motion in the newborn baby. *Proceedings of the National Academy of Sciences*, 105(2), 809–813.
- Sirigu, A., Duhamel, J. R., Cohen, L., Pillon, B., Dubois, B., & Agid, Y. (1996). The mental representation of hand movements after parietal cortex damage. *Science*, 273(5281), 1564–1568.
- Sirigu, A., Daprati, E., Ciancia, S., Giraux, P., Nighoghossian, N., Posada, A., & Haggard, P. (2004). Altered awareness of voluntary action after damage to the parietal cortex. *Nature Neuroscience*, 7(1), 80–84.
- Smith, S. M., & Nichols, T. E. (2009). Threshold-free cluster enhancement: Addressing problems of smoothing, threshold dependence and localisation in cluster inference. *NeuroImage*, 44(1), 83–98.
- Sokolov, A. A., Zeidman, P., Erb, M., Ryvlin, P., Friston, K. J., & Pavlova, M. A. (2018).
 - Structural and effective brain connectivity underlying biological motion detection. Proceedings of the National Academy of Sciences, 115(51), E12034-E12042.
 - Thurman, S. M., van Boxtel, J. J., Monti, M. M., Chiang, J. N., & Lu, H. (2016). Neural adaptation in pSTS correlates with perceptual aftereffects to biological motion and with autistic traits. Neuroimage, 136, 149-161.
 - Tsakiris, M. (2010). My body in the brain: A neurocognitive model of body-ownership. *Neuropsychologia*, 48(3), 703-712.
 - van Boxtel, J. J., & Lu, H. (2011). Visual search by action category. Journal of Vision, 11(7), 19-19.
 - van Boxtel, J. J., & Lu, H. (2012). Signature movements lead to efficient search for threatening actions. PLoS One, 7(5), e37085.
 - van Boxtel JJ, Lu H (2013) A biological motion toolbox for reading, displaying, and manipulating motion capture data in research settings. J Vis 13:7–7.
 - Verosky, S. C., & Todorov, A. (2010). Differential neural responses to faces physically similar to the self as a function of their valence. Neuroimage, 49(2), 1690-1698.
 - Vocks, S., Busch, M., Grönemeyer, D., Schulte, D., Herpertz, S., & Suchan, B. (2010). Neural correlates of viewing photographs of one's own body and another woman's body in anorexia and bulimia nervosa: An fMRI study. Journal of Psychiatry & Neuroscience, 35(3), 163-176.
 - Walbrin, J., Downing, P., & Koldewyn, K. (2019). Neural responses to visually observed social interactions. Neuropsychologia, 134, 107191.
 - Winkler AM, Ridgway GR, Webster MA, Smith SM, Nichols TE (2014) Permutation

- inference for the general linear model. Neuroimage 92: 381–397.
- Wold, A., Limanowski, J., Walter, H., & Blankenburg, F. (2014). Proprioceptive drift in the rubber hand illusion is intensified following 1 Hz TMS of the left EBA. Frontiers in Human neuroscience, 8, 390.
- Woolrich MW, Behrens TE, Beckmann CF, Jenkinson M, Smith SM (2004) Multilevel linear modelling for FMRI group analysis using Bayesian inference. Neuroimage 21:1732–1747.
- Woolrich MW, Jbabdi S, Patenaude B, Chappell M, Makni S, Behrens T, Beckmann C, Jenkinson M, Smith SM (2009) Bayesian analysis of neuro- imaging data in FSL. Neuroimage 45:S173–S186.
- Worsley KJ (2001) Statistical analysis of activation images. In: Functional MRI: an introduction to methods, Vol. 14, pp 251–270.
- Wurm, M. F., Hrkać, M., Morikawa, Y., & Schubotz, R. I. (2014). Predicting goals in action episodes attenuates BOLD response in inferior frontal and occipitotemporal cortex. Behavioural brain research, 274, 108-117.
- Zimmermann, M., Toni, I., & de Lange, F. P. (2018). Body posture modulates action perception. Journal of Neuroscience, 33(14), 5930-5938.

Declaration of Competing Interest

S.N. is an employee of Google DeepMind. Google DeepMind had no role in study design, data collection and analysis, decision to publish, or preparation of the manuscript. All other authors declare no competing financial interests.